ISSN 1674-1056
http://cpb.iphy.ac.cn
http://iopscience.iop.org/cpb
中国物理 B
Chinese Physics
中国物理 Chinese Physics B

Mg acceptor activation mechanism and hole transport characteristics in highly Mg-doped AlGaN alloys

Qing-Jun Xu(徐庆君), Shi-Ying Zhang(张士英), Bin Liu(刘斌), Zhen-Hua Li(李振华), Tao Tao(陶涛), Zi-Li Xie(谢自力), Xiang-Qian Xiu(修向前), Dun-Jun Chen(陈敦军), Peng Chen(陈鹏), Ping Han(韩平), Ke Wang(王科), Rong Zhang(张荣), You-Dou Zheng(郑有炓)

Citation: Chin. Phys. B . 2020, 29(5): 058103 . **doi:** 10.1088/1674-1056/ab7e93
Journal homepage: http://cpb.iphy.ac.cn; http://iopscience.iop.org/cpb

What follows is a list of articles you may be interested in

Magnesium incorporation efficiencies in $Mg_xZn_{1-x}O$ films on ZnO substrates grown by metalorganic chemical vapor deposition

Qi-Chang Hu(胡启昌), Kai Ding(丁凯)

Chin. Phys. B . 2017, 26(6): 068104 . **doi:** 10.1088/1674-1056/26/6/068104

Effects of Mg doping in the quantum barriers on the efficiency droop of GaN based light emitting diodes

Yang Liu(刘扬), Yongchun Yang(杨永春)

Chin. Phys. B . 2016, 25(5): 058101 . **doi:** 10.1088/1674-1056/25/5/058101

Control of symmetric properties of metamorphic $In_{0.27}Ga_{0.73}As$ layers by substrate misorientation

Shu-Zhen Yu(于淑珍), Jian-Rong Dong(董建荣), Yu-Run Sun(孙玉润), Kui-Long Li(李奎龙),Xu-Lu Zeng(曾徐路), Yong-Ming Zhao(赵勇明), Hui Yang(杨辉)

Chin. Phys. B . 2016, 25(3): 038101 . **doi:** 10.1088/1674-1056/25/3/038101

Nanodots and microwires of ZrO_2 grown on $LaAlO_3$ by photo-assisted metal-organic chemical vapor deposition

Feng Guo(郭峰), Xin-Sheng Wang(汪薪生), Shi-Wei Zhuang(庄仕伟), Guo-Xing Li(李国兴), Bao-Lin Zhang(张宝林), Pen-Chu Chou(周本初)

Chin. Phys. B . 2016, 25(2): 028103 . **doi:** 10.1088/1674-1056/25/2/028103

L_g=100 nm T-shaped gate AlGaN/GaN HEMTs on Si substrates with non-planar source/drain regrowth of highly-doped n^+-GaN layer by MOCVD

Huang Jie, Li Ming, Tang Chak-Wah, Lau Kei-May

Chin. Phys. B . 2014, 23(12): 128102 . **doi:** 10.1088/1674-1056/23/12/128102

Mg acceptor activation mechanism and hole transport characteristics in highly Mg-doped AlGaN alloys*

Qing-Jun Xu(徐庆君)[1,2,†], Shi-Ying Zhang(张士英)[1,2,†], Bin Liu(刘斌)[1,‡], Zhen-Hua Li(李振华)[1,2], Tao Tao(陶涛)[1], Zi-Li Xie(谢自力)[1,§], Xiang-Qian Xiu(修向前)[1], Dun-Jun Chen(陈敦军)[1], Peng Chen(陈鹏)[1], Ping Han(韩平)[1], Ke Wang(王科)[1], and Rong Zhang(张荣)[1], and You-Liao Zheng(郑有炓)[1]

[1] *Key Laboratory of Advanced Photonic and Electronic Materials, School of Electronic Science and Engineering, Nanjing University, Nanjing* 210093, *China*
[2] *College of Optoelectronics Engineering, Zaozhuang University, Zaozhuang* 277160, *China*

(Received 15 October 2019; revised manuscript received 25 January 2020; accepted manuscript online 11 March 2020)

The Mg acceptor activation mechanism and hole transport characteristics in AlGaN alloy with Mg doping concentration ($\sim 10^{20}$ cm^{-3}) grown by metal–organic chemical vapor deposition (MOCVD) are systematically studied through optical and electrical properties. Emission lines of shallow oxygen donors and $(V_{III}$ complex$)^{1-}$ as well as V_N^{3+} and neutral Mg acceptors are observed, which indicate that self-compensation is occurred in Mg-doped AlGaN at highly doping levels. The fitting of the temperature-dependent Hall effect data shows that the acceptor activation energy values in Mg-doped $Al_xGa_{1-x}N$ ($x = 0.23$, 0.35) are 172 meV and 242 meV, and the hole concentrations at room temperature are 1.2×10^{18} cm^{-3} and 3.3×10^{17} cm^{-3}, respectively. Therefore, it is believed that there exists the combined effect of the Coulomb potentials of the dopants and screening of the Coulomb potentials by a high hole concentration. Moreover, due to the high ionized acceptors' concentration and compensation ratio, the impurity conduction becomes more prominent and the valence band mobility drops sharply at low temperature.

Keywords: AlGaN, Mg doping, MOCVD, cathodo-luminescence, Hall measurement

PACS: 81.05.Ea, 82.33.Ya, 81.15.Gh, 78.60.Hk **DOI:** 10.1088/1674-1056/ab7e93

1. Introduction

Aluminum–gallium–nitride (AlGaN) alloy is recognized as one of most promising materials for applications in deep ultraviolet (DUV) light emitting diode (LED) devices,[1–3] due to their great potential applications in sterilization, water purification, and biological and chemical agent detection.[4,5] In order to fabricate high efficiency DUV-LEDs, it is required to obtain a highly conductive p-type AlGaN layer with a high AlN mole fraction. However, since the ionization energy for Mg-doped $Al_xGa_{1-x}N$ alloys dramatically increases with AlN mole fraction increasing from 170 meV (for $x = 0$) to 630 meV (for $x = 1$),[6,7] which leads to very small hole concentration in the valence band at room-temperature. Therefore it is rather difficult to achieve highly conductive p-type AlGaN.

Recently, very high Mg-doped level (around 10^{20} cm^{-3}–10^{21} cm^{-3}) could be adopted to obtain adequate free hole conductivity, because of the low activation ratio of holes in AlGaN with high AlN mole fraction.[8] But high doping effect easily leads to the valence band-tail states and impurity band to form.[9] In addition, since the formation energy values of intrinsic defects and their complexes are significantly reduced in highly p-type Al-rich AlGaN alloys, these defects could further compensate for the presence of free holes.[10,11] So the fundamental understanding of the impurity transitions, as well as Mg acceptor activation mechanism and hole transport characteristics in highly Mg-doped AlGaN has become increasingly important.

In this paper, we systematically investigate the optical transitions of impurity transitions and variable-temperature Hall effect to clarify the Mg acceptor activation mechanism and transport characteristics in highly Mg-doped AlGaN alloys. The optical characteristics of undoped AlGaN and Mg-doped AlGaN alloys are investigated by using the cathodo-luminescence (CL). The electrical properties of each sample

*Project supported by the National Key Research and Development Program of China (Grant Nos. 2017YFB0403100 and 2017YFB0403101), the National Natural Science Foundation of China (Grant Nos. 61704149, 61674076, and 61605071), the Natural Science Foundation of Jiangsu Province , China (Grant Nos. BY2013077, BK20141320, and BE2015111), the Project of Science and Technology Development Program in Shandong Province, China (Grant Nos. 2013YD02054 and 2013YD02008), the Project of Shandong Provincial Higher Educational Science and Technology Program, China (Grant No. J13LN08), the Collaborative Innovation Center of Solid State Lighting and Energy-saving Electronics, Priority Academic Program Development of Jiangsu Higher Education Institutions (PAPD), the Six-Talent Peaks Project of Jiangsu Province, China (Grant No. XYDXX-081), the Open Fund of the State Key Laboratory on Integrated Optoelectronics, China (Grant No. IOSKL2017KF03), the Project of Autonomous Innovation and Achievement Transformation Program in Zaozhuang City, China (Grant No. 2017GH3), the Overseas Study Program Funded by Shandong Provincial Government, China, the Laboratory Open Fund from Jiangsu Key Laboratory of Photoelectric Information Functional Materials, China, and the Doctoral Foundation Project of Zaozhuang University, China.

†These authors contributed equally to this work.
‡Corresponding author. E-mail: bliu@nju.edu.cn
§Corresponding author. E-mail: xzl@nju.edu.cn

© 2020 Chinese Physical Society and IOP Publishing Ltd

are analyzed by using the temperature-dependent Hall effect measurements. It is discovered that there exists a pronounced reduction activation energy for Mg acceptor and lower hole mobility in highly Mg-doped AlGaN alloys, due to the high ionized acceptor concentration and compensation ratio.

2. Experimental procedures

The unintentionally doped and Mg-doped AlGaN alloys were grown by metal–organic chemical vapor deposition (MOCVD) using trimethylaluminum (TMAl), trimethylgallium (TMGa), ammonia (NH_3) as the organometallic precursors for Al, Ga, and N, respectively. Hydrogen (H_2) was used as the carrier gas. For Mg doping, an optimized molar flux of biscyclopentadienyl-magnessium (Cp_2Mg) at 4.8×10^{-7} mol/min was used. More detailed growth procedures for undoped and Mg-doped $Al_xGa_{1-x}N$ alloys were reported in Refs. [12,13]. The AlN mole fractions of AlGaN samples were determined by high-resolution x-ray diffraction (HRXRD) through using Cu K line = 0.15406 nm radiation (PANalytical X'Pert Pro XRD). The concentration of Mg atoms incorporated into Mg-doped AlGaN alloys was determined to be 1×10^{20} cm^{-3} by using secondary ion mass spectrometry (SIMS).[13] The optical properties were characterized by cathodo-luminescence spectra (CL, Gatan Mono CL3+) at low temperature $\sim$ 120 K. Post growth rapid thermal annealing in N_2 ambient was used to activate Mg acceptor. The electrical properties were measured by variable-temperature Hall effect measurement through using the van der Pauw method (Accent HL5500 measurement system).

3. Results and discussion

Figure 1 shows the comparison between the CL spectra measured at the low temperature (120 K) for undoped and highly Mg-doped $Al_xGa_{1-x}N$ alloys of varying x (0.23, 0.35, and 0.57). The band edge transitions are at 3.955 eV, 4.161 eV, and 4.566 eV for the undoped $Al_xGa_{1-x}N$ (x = 0.23, 0.35, and 0.57) alloys, respectively, due to the free excition (FX) transition.[14] In additon, it is observed that the peak energy position of impurity transition, denoted as $(DAP)_I$ shifts from 3.642 eV for x = 0.23 to 4.146 eV for x = 0.57, since the Si, O, and C impurities are easily incorporated during MOCVD growth.[15]

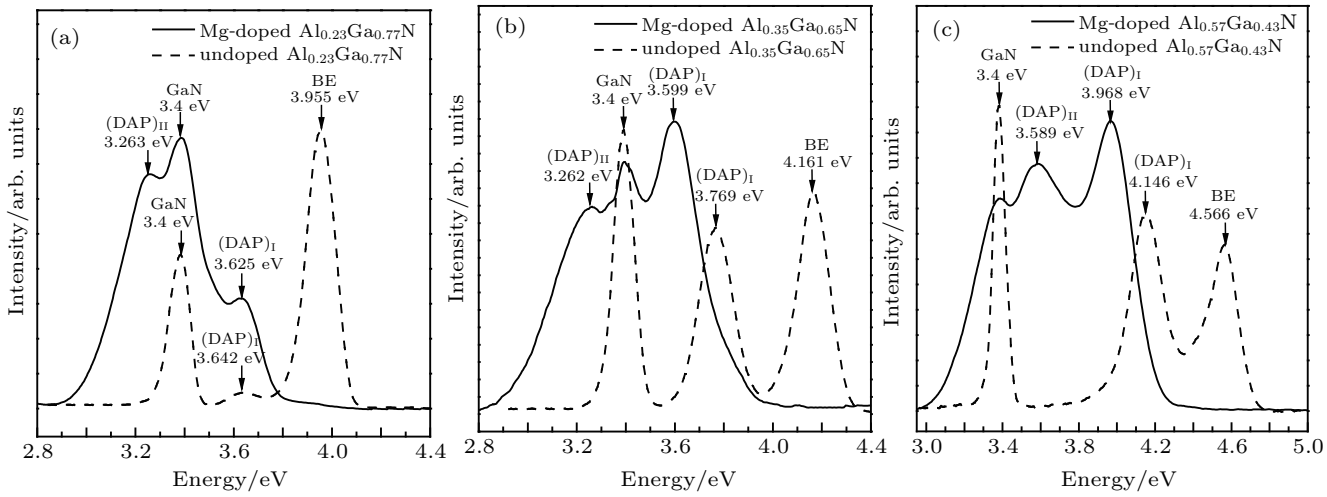


Fig. 1. Low-temperature (120 K) CL spectra of undoped and highly Mg-doped $Al_xGa_{1-x}N$ alloys with varying x (0.23, 0.35, and 0.57) with dashed lines and solid lines denoting undoped and Mg-doped samples, respectively.

Figure 2(a) shows the plots of the CL spectral peak position (E_{emi}) *versus* AlN mole fraction (x) of the above impurity transitions in undoped AlGaN alloys together with those of cation vacancy complexes with one-negative charge $(V_{III}\text{-complex})^{-1}$ related transitions. The energy position of these impurity transitions show a continuous increase with AlN mole fraction increasing. Correlating the onset of much oxygen concentration in SIMS results,[13] we suggest that the presently observed impurity transition shown in undoped AlGaN alloys is also attributed to the recombination between electrons bound to oxygen donors and $(V_{III}\text{-complex})^{-1}$, such as $(V_{Ga}\text{-}2O_N)^{1-}$.

To obtain a more comprehensive picture of O donor and $(V_{III}\text{-complex})^{-1}$ acceptor energy levels in undoped AlGaN alloy, we plot its donor, acceptor energy levels, conduction (E_c), and valence (E_v) band edges *versus* AlN mole fraction x in Fig. 2(b). Now, the ionization energy value of the O donor (E_D) is assumed to increase linearly from 25 meV to 86 meV with x increasing from 0 to 1 in $Al_xGa_{1-x}N$ alloys,[17,18] and the peak position of band edge transition for undoped AlGaN alloy is considered, other parameters and the same procedure are used as described in Ref. [16]. The Coulomb interaction between the ionized donors and acceptors is neglected. The acceptor level (E_A) in undoped $Al_xGa_{1-x}N$ alloys as a func-

tion of AlN mole fraction x could be written as

$$E_{\rm A} = E_{\rm g}(x) - E_{\rm emi} - E_{\rm D} + E_{\rm v}, \quad (1)$$

where $E_{\rm g}(x)$ is the bandgap of AlGaN alloys, $E_{\rm v} = -0.3\Delta E_{\rm g}(x), E_{\rm c} = E_{\rm g}({\rm GaN}) + 0.7\Delta E_{\rm g}(x)$, and $E_{\rm D}$ is the O donor energy level.[16] $E_{\rm A}$ is plotted in Fig. 2(b) together with $E_{\rm c}$ and $E_{\rm v}$ as a function of x, which clearly shows that the $E_{\rm A}$ of deep acceptor $(V_{\rm III}\text{-complex})^{1-}$ is a horizontal line for the entire AlGaN alloy range.

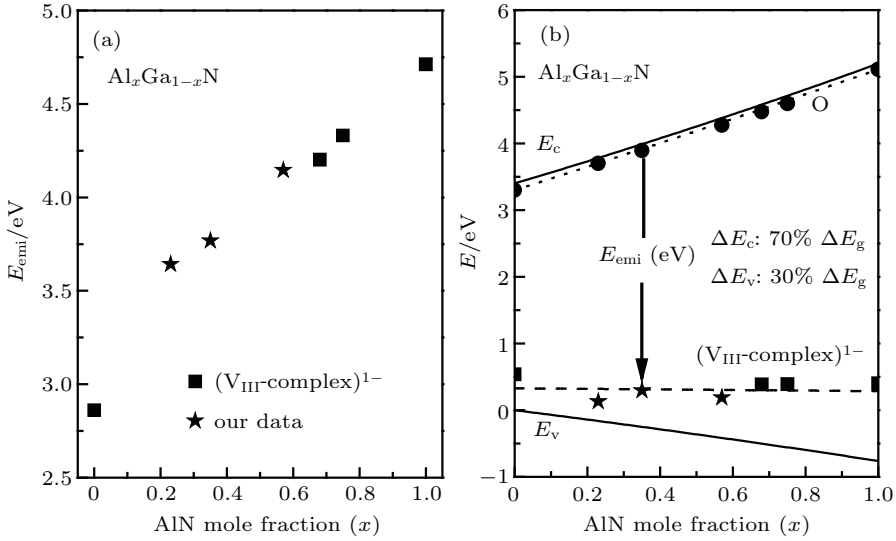


Fig. 2. (a) CL peak position ($E_{\rm emi}$) of present impurity transition (solid stars) observed from Fig. 1 and those of $(V_{\rm III}$ complex$)^{1-}$ related transitions (solid squars) obtained from undoped $Al_xGa_{1-x}N$ alloys as a function of AlN mole fraction x in Ref. [16]; (b) $E_{\rm A}$ *versus* AlN mole fraction for $(V_{\rm III}\text{-complex})^{1-}$, $E_{\rm v}$, $E_{\rm c}$, and $E_{\rm D}$.

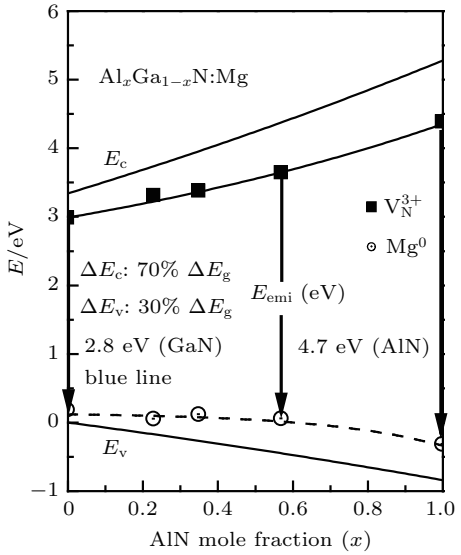


Fig. 3. Plots of energy levels ($E_{\rm A}$, $E_{\rm D}$) of acceptor and donor with conduction and valence band edge ($E_{\rm c}$, $E_{\rm v}$) *versus* AlN mole fraction (x) in Mg-doped $Al_xGa_{1-x}N$ alloys.

For Mg-doped AlGaN alloys, the band edge transitions become completely quenched asindicated by the solid line of Fig. 1. Compared with those in undoped samples, $(DAP)_{\rm I}$ in Mg-doped samples has a slightly lower energy position, which is usually ascribed to the fact that the Mg incorporation makes the magnitude of the strain changed slightly.[19] The emission lines at 3.263 eV, 3.262 eV, and 3.589 eV are dominant for Mg-doped $Al_xGa_{1-x}N$ alloys ($x = 0.23$, 0.35, and 0.57), respectively, which do not occur in undoped AlGaN alloys. So those emissions are attributed to Mg impurity-related transitions. Since the formation energy of the nitrogen vacancy with three positive charges (V_N^{3+}) is small, it is suggested that the positive charges (V_N^{3+}) be the most dominant compensating centers in Mg-doped $Al_xGa_{1-x}N$ alloys.[6,10] Therefore, we suggest that the physical origin of those emission lines is consistent with that of the 2.8-eV line in Mg-doped GaN[20–25] and the 4.7-eV line in Mg-doped AlN,[6,26] which is ascribed to the recombination of electrons bound to V_N^{3+} and neutral Mg acceptors, denoted as $(DAP)_{\rm II}$.[27] Similarly, we further investigate the energy levels ($E_{\rm A}$, $E_{\rm D}$) of acceptor and donor with conduction and valence band edge ($E_{\rm c}$, $E_{\rm v}$) *versus* AlN mole fraction (x) in Mg-doped $Al_xGa_{1-x}N$ alloys as shown in Fig. 3. The spectral peak position ($E_{\rm emi}$) of impurity transition, together with 2.8-eV line in Mg-doped GaN and 4.7-eV line in Mg-doped AlN is also plotted for $Al_xGa_{1-x}N$ alloys as a function of x. Based on the Hall effect measurement results and reported Mg acceptor levels,[6] the V_N^{3+} energy levels have been deduced in Mg-doped $Al_xGa_{1-x}N$ in the whole range of AlN mole fraction.[27]

In order to characterize the ionization of Mg acceptor, we carry out the temperature-dependent Hall effect measurements. The resistivity for Mg-doped $Al_{0.57}Ga_{0.43}N$ alloy is highly resistive (not shown), which is most likely to be due to the resistivity exponentially increasing with the activation energy ($E_{\rm A}$), and being compensated for by nitrogen vacancies (as shown in Fig. 1). So the temperature range where Hall measurements are performed is not large enough to determine $E_{\rm A}$ for Mg-doped $Al_{0.57}Ga_{0.43}N$ alloy. Figure 4(a)

shows the temperature-depenmdent resistivity curves of Mg-doped $Al_xGa_{1-x}N$ ($x = 0.23$ and 0.35) alloys. In Mg-doped $Al_{0.23}Ga_{0.77}N$ alloys, the resistivity is almost constant at temperatures ranging from 200 K to 325 K, then it decreases with the temperature increasing from 325 K to 650 K, which clearly indicates that there exist two different hole transport mechanisms. However, the resistivity decreases exponentially by more than one order of magnitude in Mg-doped $Al_{0.35}Ga_{0.65}N$ alloys, while the temperature is increased from 260 K to 535 K.

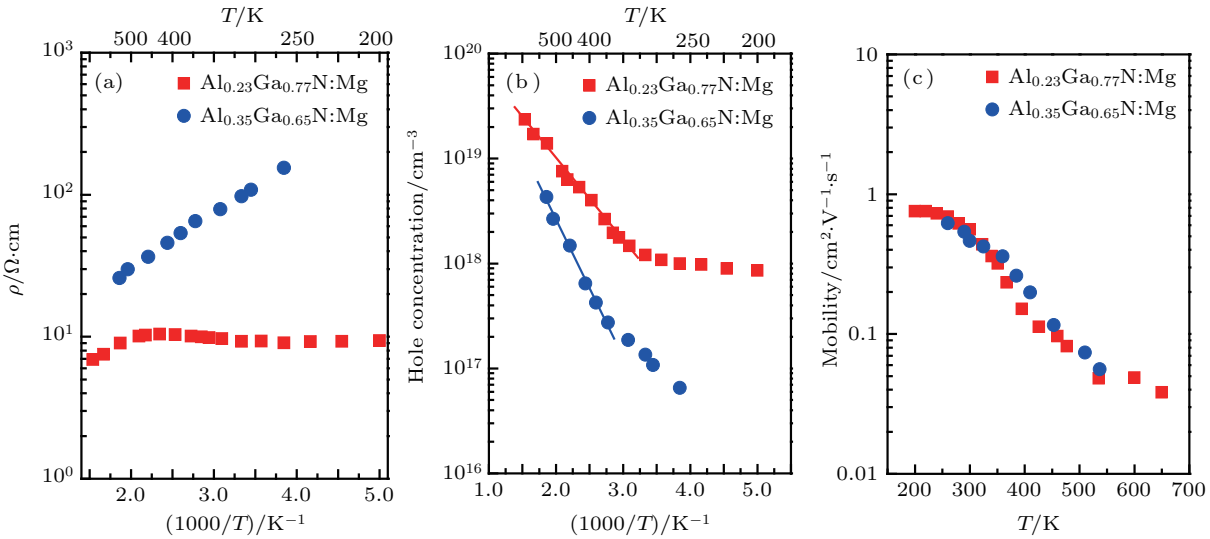


Fig. 4. Temperature-dependent (a) resistivity, (b) hole concentration, and (c) mobility of Mg-doped $Al_xGa_{1-x}N$ ($x = 0.23$ and 0.35). Solid lines are obtained from Arrhenius plots in high-temperature region.

Since the resistivity includes the contributions from both hole concentration (p) and mobility (μ), we evaluate the E_A values of Mg acceptors for Mg-doped $Al_xGa_{1-x}N$ ($x = 0.23$ and 0.35) based on the temperature-dependent free hole concentration as shown in Fig. 4(b). In Mg-doped $Al_{0.23}Ga_{0.77}N$ alloys, the hole concentration exhibits an increasing trend with temperature increasing. But the hole concentration is insensitive to temperature in a lower temperature range from 200 K to 325 K, and E_A calculated from Arrhenius plots is 17 meV, indicating the onset of impurity band conduction.[8,28,29] Thus, holes need not to occupy valence band states for carrier transport.[30]

For the Mg-doped $Al_{0.35}Ga_{0.65}N$ alloys, the hole concentration also increases with temperature increasing due to the thermal ionization of Mg dopants. There exists a deviation between the experimental measurement data and the fitting curve at temperatures ranging from 260 K to 360 K, which implies that the thermal activation of holes starts to play a role. But only temperature above 360 K, the thermal activation becomes dominant for the hole transport mechanism. The fitting lines are obtained by the following Eqs. (2) and (3) based on the charge neutrality condition

$$\frac{p(p+N_D)}{N_A - N_D - p} = \frac{N_V}{g}\exp\left(-\frac{E_A}{k_B T}\right), \tag{2}$$

$$N_V = 2(2\pi m_h^* k_B T)^{3/2}/h^3, \tag{3}$$

where p, E_A, N_A, and N_D are the hole concentration, the acceptor activation energy, the acceptor, and donor concentrations, respectively; g is the acceptor degeneracy factor, which is assumed to be equal to four for the AlGaN band structure; T is the temperature; k_B is the Boltzmann constant; and h is the Planck's constant; N_V is the effective valence band density of states; the hole effective mass (m_h^*) of AlGaN are changed with the linear interpolation between the effective mass of AlN and GaN.[31] The values of E_A, N_A, N_D, and the compensation ratio N_D/N_A are listed in Table 1.

Table 1. Fitting results from variable Hall measurements of the Mg-doped $Al_xGa_{1-x}N$ ($x = 0.23$ and 0.35) alloys.

AlN mole fraction	N_A/cm^{-3}	N_D/cm^{-3}	Compensition ratio/%	E_A/meV	ΔE_A/meV	E_{A0}/meV
0.23	4.45×10^{20}	1.42×10^{19}	3.2%	172	79	251
0.35	1.68×10^{20}	6.89×10^{18}	4.1%	242	63	305

The values of activation energy (E_A) are 172 meV and 242 meV for Mg-doped $Al_{0.23}Ga_{0.77}N$, and $Al_{0.35}Ga_{0.65}N$, respectively, which are lower than the previously estimated value of of E_A as a function of the AlN mole fraction in Mg-doped AlGaN alloys.[6] The lowering of the value of the activation energy (ΔE_A) is ascribed to the combined effect of the Coulomb potentials of the Mg dopants and the screening of the Coulomb potentials by a high concentration of free holes. Moreover, ΔE_A is assumed to be proportional to the average distance $(N_A^-)^{1/3}$ between ionized acceptors.[32]

Thus, the acceptor activation energy may be expressed as

$$E_{\rm A}(N_{\rm A}^-) = E_{\rm A0} - \Delta E_{\rm A} = E_{\rm A0} - f(N_{\rm A}^-)^{1/3}, \\ = E_{\rm A0} - f\cdot(p+N_{\rm D})^{1/3}, \quad (4)$$

$$f = \Gamma\left(\frac{2}{3}\right)\left(\frac{4\pi}{3}\right)^{1/3}\frac{q^2}{4\pi\varepsilon_{\rm s}}. \quad (5)$$

Here, $E_{\rm A0}$ is the activation energy at $T=0$ while the concentration of ionized acceptors is sufficiently low; q is the electronic charge; $\varepsilon_{\rm s}$ is the dielectric constant ($9.5\varepsilon_0$); $N_{\rm A}$, $N_{\rm D}$, and $\Delta E_{\rm A}$ are given by Eqs. (4) and (5); the values of $E_{\rm A0}$ can be obtained, which is consistent with typically reported Mg activation energy.[6] So it is reasonable to explain that the p-type conduction mainly results from the hole carriers thermally excited from the Mg acceptors at temperatures higher than 325 K and 360 K for the Mg-doped $Al_xGa_{1-x}N$ ($x=0.23$ and 0.35), respectively. This similar electrical transport characteristics has been observed in Mg-doped InGaN,[33] GaN,[8] and AlGaN.[29] The transition temperature increases as the bandgap energy become larger, *i.e.*, 250 K for Mg-doped InGaN and GaN and 500 K for Mg-doped $Al_{0.7}Ga_{0.3}N$. Figure 4(c) shows the measured hole mobilities varying with temperature. The mobility values of two samples monotonically increase with temperature decreasing, which implies the possibility of acoustic phonon scattering.[34] Moreover, two samples have relatively low mobility around 0.5 $cm^2/V{\cdot}s$ at room temperature, which could be explained by the ionized impurity scattering caused by Mg acceptors and compensating donors.[35]

4. Conclusions

In this work, the optical and electrical characteristics of highly Mg-doped $Al_xGa_{1-x}N$ alloys ($0.23\leq x\leq 0.57$) are investigated. Their cathodo-luminescence spectra show that there exist two groups of impurity transitions in Mg-doped AlGaN alloys: one is assigned to the recombination between electrons bound to shallow oxygen donors and $(V_{III}\text{-complex})^{1-}$, and the other is the recombination of electrons bound between V_N^{3+} and neutral Mg acceptors, which indicates that there exists the obvious self-compensation phenomenon in Mg-doped AlGaN alloy. The values of effective acceptor activation energy ($E_{\rm A}$) in Mg-doped $Al_xGa_{1-x}N$ films ($x=0.23$ and 0.35) are determined to be 172 meV and 242 meV, and the hole concentrations are 1.2×10^{18} cm^{-3} and 3.3×10^{17} cm^{-3} at room temperature, respectively. It is important to consider the Coulomb interaction between ionized acceptors, which reduces the activation energy due to increasing the degree of ionization and compensation ratio. Furthermore, the other high doping effects are also observed, including impurity conduction and lower hole mobility.

References

[1] Wang L Y, Song W D, Hu W X, Li G, Luo X J, Wang H, Xiao J K, Guo J Q, Wang X F, Hao R, Yi H X, Wu Q B and Li S T 2019 *Chin. Phys. B* **28** 018503

[2] Liu B, Zhang R, Xie Z L, Liu Q J, Zhang Z, Li Y, Xiu X Q, Yao J, Mei Q, Zhao H, Han P, Lu H, Chen P, Gu S L, Shi Y, Zheng Y D, Cheung W Y, Ke N and Xu J B 2008 *J. Cryst. Growth* **310** 4499

[3] Zhang J P, Wu S, Rai S, Mandavilli V, Adivarahan V, Chitnis A, Shatalov M and Asif Khan M 2003 *Appl. Phys. Lett.* **83** 3456

[4] Liang Y H and Towe E 2018 *Appl. Phys. Rev.* **5** 011107

[5] Li D B, Jiang K, Sun X J and Guo C L 2018 *Adv. Opt. Photon.* **10** 43

[6] Katsuragawa M, Sota S, Komori M, Anbe C, Takeuchi T, Sakai H, Amano H and Akasaki I 1998 *J. Cryst. Growth* **189/190** 528

[7] Jiang H X and Lin J Y 2014 *Semicond. Sci. Technol.* **29** 84003

[8] Kozodoy P, Xing H L, DenBaars S P, Mishra U K, Saxler A, Perrin R, Elhamri S and Mitchel W C 2000 *J. Appl. Phys.* **87** 1832

[9] Schubert E F 1993 *Doping in* III–V *Semiconductors* (Cambridge: University Press)

[10] Stampfl C and Van de Walle C G 2002 *Phys. Rev. B* **65** 155212

[11] Van de Walle C G and Neugebauer J 2004 *J. Appl. Phys.* **95** 3851

[12] Xu Q J, Liu B, Zhang S Y, Tao T, Dai J P, He G T, Xie Z L, Xiu X Q, Chen D J, Chen P, Han P and Zhang R 2017 *Superlattice. Microst.* **101** 144

[13] Xu Q J, Zhang S Y, Liu B, Tao T, Xie Z L, Xiu X Q, Chen D J, Chen P, Han P, Zheng Y D and Zhang R 2018 *Superlattice. Microst.* **119** 150

[14] Nepal N, Nakarmi M L, Nam K B, Lin J Y and Jiang H X 2004 *Appl. Phys. Lett.* **85** 2271

[15] Gu C J, Stevie F A, Hitzman C J, Saripalli Y N, Johnson M and Griffis D P 2006 *Appl. Surf. Sci.* **252** 7228

[16] Nepal N, Nakarmi M L, Lin J Y and Jiang H X 2006 *Appl. Phys. Lett.* **89** 092107

[17] Taniyasu Y, Kasu M and Kobayashi N 2002 *Appl. Phys. Lett.* **81** 1255

[18] Nakarmi M L, Kim K H, Zhu K, Lin J Y and Jiang H X 2004 *Appl. Phys. Lett.* **85** 3769

[19] Feng Q, Wang F X and Hao Y 2004 *Acta Phys. Sin.* **53** 3587 (in Chinese)

[20] Shahedipour F and Wessels B W 2000 *Appl. Phys. Lett.* **76** 3011

[21] Kaufmann U, Kunzer M, Maier M, Obloh H, Ramakrishnan A, Santic B and Schlotter P 1998 *Appl. Phys. Lett.* **72** 1326

[22] Kaufmann U, Kunzer M, Obloh H, Maier M, Manz Ch, Ramakrishnan A and Santic B 1999 *Phys. Rev. B* **59** 5561

[23] Kwon Y H, Shee S K, Gainer G H, Park G H, Hwang S J and Song J J 2000 *Appl. Phys. Lett.* **76** 840

[24] Reshchikov M A, Yi G C and Wessels B W 1999 *Phys. Rev. B* **59** 13176

[25] Shahedipour F and Wessels B W 2001 *MRS Internet J. Nitride Semicond. Res.* **6** 12

[26] Nakarmi M L, Nepal N, Ugolini C, Altahtamouni T M, Lin J Y and Jiang H X 2006 *Appl. Phys. Lett.* **89** 152120

[27] Nakarmi M L, Nepal N, Lin J Y and Jiang H X 2009 *Appl. Phys. Lett.* **94** 091903

[28] Simpkins B S, Pehrsson P E and Laracuente A R 2006 *Appl. Phys. Lett.* **88** 072111

[29] Kinoshita T, Obata T, Yanagi H and Inoue S I 2013 *Appl. Phys. Lett.* **102** 012105

[30] Gong Y, Gu Y, Kuskovsky Igor L, Neumark G F, Li J, Lin J Y, Jiang H X and Ferguson I 2004 *Mat. Res. Soc. Symp. Proc.* 798 Y5.16.1

[31] Suzuki M, Uenoyama T and Yamase A 1995 *Phys. Rev. B* **52** 8132

[32] Götz W, Kern R S, Chen C H, Liu H, Steigerwald D A and Fletcher R M 1999 *Mater. Sci. Eng. B* **59** 211

[33] Kumakura K, Makimoto T and Kobayashi N 2003 *J. Appl. Phys.* **93** 3370

[34] Costato M, Gagliani G, Jacoboni C and Reggiani L 1974 *J. Phys. Chem. Solids* **35** 1605

[35] Horita M, Takashima S, Tanaka R, Matsuyama H, Ueno K, Edo M, Takahashi T, Shimizu M and Suda J 2017 *Jpn. J. Appl. Phys.* **56** 031001